

Effects of injection timing on performance and droplet characteristics of a sixteen-valve four cylinder engine

S. Chappuis, B. Cousyn, M. Posylkin, F. Vannobel, J. H. Whitelaw

336

Abstract The performance and droplet characteristics of a sixteen-valve, four cylinder engine operating with combustion in one cylinder have been measured with part load, a speed of 1200 rpm and a stoichiometric mixture of gasoline and air. The indicated mean-effective cylinder pressure was found to be constant with initiation of injection from 150° to 630° of crank angle after top-dead-centre of intake and with a 10% reduction between 30° and 60° which coincided with maxima in the covariance in pressure and in the emissions of unburned hydrocarbon. There was also a tendency for performance to decline with injection after 660° .

Measurements with laser- and phase-Doppler velocimeters showed that the number of droplets entering the cylinder was much reduced with injection at crank angles corresponding to closed inlet valves due to evaporation, and that the few large droplets which emerged did not survive until top-dead-centre of compression. In contrast, some of the many droplets associated with injection with the valves open survived to the crank angle of ignition and it is likely that these led to an inhomogeneous charge with poorer flame-front propagation responsible for reduction in performance.

1 Introduction

It is well known that the performance of port-injected engines depends on the timing of injection and particular choices have been made for the many engines which are in use today. The engine management system is arranged to alter the quantity

and time of fuel injection to cope with the different conditions required of the engine and the parameters are based mainly on bench tests and normal operation. At the same time, the geometry of the port and cylinder head allow some control of the flow conditions at the time of ignition including combinations of swirl and tumble, and their consequences for mean motion and velocity fluctuations in the vicinity of the spark gap as explored, for example, by Arcoumanis et al. (1991).

The emphasis of the present contribution is on quantification of the performance of a 16-valve, four cylinder engine as a function of injection timing and the relationships between the maximum and indicated mean-effective pressures, drivability, emissions of unburned hydrocarbon and the droplet characteristics in the cylinder. It follows from previous investigations in a eight-valve, four cylinder engine, Vannobel et al. (1994), Posylkin et al. (1994) and Cousyn et al. (1995) which showed that droplets of fuel entered the engine from the inlet valve in a cone of increasing diameter, with droplet number density and droplet size ranges dependent on injection timing. Cousyn et al. (1995) also demonstrated that the results obtained with one cylinder and four cylinders operating were little different and with identical trends, and this result justifies the use of the present four cylinder engine with combustion in one cylinder. Reference will be made to these investigations in the considerations of the present results and also to those in simplified geometries of Posylkin et al. (1995a, b).

Previous investigations of the influence of injection timing on the performance of engines with four valves per cylinder include those of Mikulic et al. (1990) and Alkidas (1994) and were concerned with stoichiometric burning as in the present investigation. In general, the symmetry of the four-valve cylinder head precludes the introduction of swirl unless the timing and lift of the two inlet valves are arranged to be different and this was not done in these investigations which did, however, benefit from the mean motion and fluctuations caused by the breakdown of tumbling vortices. The results of these investigation showed the best performance was obtained with injection with inlet the valves closed, whereas injection timing which corresponded to open inlet valves resulted in poor drivability, lower power output and high emissions of unburned hydrocarbon due to the inhomogeneity of the charge in the cylinder. It is of interest that similar results were obtained by Winklhofer et al. (1992) and Bandel et al. (1989) who conducted experiments with two-valve engines operated with lean mixtures. In addition, the latter paper confirmed that port-generated swirl improved combustion performance with open-valve injection.

Received: 19 February 1996/Accepted: 8 October 1996

S. Chappuis, B. Cousyn, F. Vannobel
Peugeot S. A. DRAS/RMP, Route de Gisy, Velizy F-78140 France

M. Posylkin, J. H. Whitelaw
Thermofluids Section, Department of Mechanical Engineering,
Imperial College of Science, Technology and Medicine,
London SW7 2BX England

Correspondence to: J. H. Whitelaw

The authors are glad to acknowledge financial support from the European Union, Contract JOU2-CT92-0162 and considerable assistance from the staff of Peugeot S.A., particularly F. Galliot and F. Neveu. The assistance of M Migl in final part of the experimental programme was also greatly appreciated. The technician staff of the Thermofluids Section were essential to the arrangement and maintenance of the engine.

Similarly, in the operation of their four-valve single cylinder engine with different schedules for the two inlet valves to produce a swirl ratio of about 2.5, Horie et al. (1992) found that the engine operated with good drivability, low emissions of NO_x and air-fuel ratios in excess of 22 and Hardalupas et al. (1995) performed detailed in-cylinder experiments to explain the relationship of performance to fuel preparation and, thereby, to provide a basis for operation at leaner conditions. It was concluded that the combination of injection of fuel with the valves open and the angled tumble vortex to transport them towards the spark gap, led to a region of richer mixture at the spark gap at the time of ignition. The more fundamental investigations of Arcoumanis et al. (1994, 1996) have shown that a flame which propagates initially in a region of rich mixture can continue into a lean region to allow acceptable concentrations of unburned hydrocarbon at overall air-fuel ratios in excess of 40. The present investigation provides information relevant to lean-burn operation, though based on experiments with stoichiometric mixtures, and this will be considered in the Discussion of the present droplet results.

The engine is described in the following section together with instrumentation and its operation. The results are presented in the two parts of section three which are concerned respectively with engine performance, and the nature of the spray in atmospheric air and within the cylinder under firing conditions. The final section provides summary conclusions and their implications for engine operation outside the range of the present conditions.

2 Engine and instrumentation

The experiments were carried out with a two litre, four stroke, four cylinder spark ignition engine (PSA model XU10J4R) with the specifications of Table 1. The engine was a production model with port injection, four valves per cylinder, and a combustion chamber with a pent roof. Modifications were required to allow optical access to one of the cylinders which was the only one fired during the experiments. Previous experiments of Cousyn et al. (1995) in a two-valve engine had shown that an engine which operated with combustion in one cylinder can provide conditions typical of multi-cylinder engine, at least for investigation of droplet characteristics. The crankshaft of the engine was coupled to a 15 kW DC motor

Table 1. Engine specifications PSA XU10J4R

Type	4 stroke, 4 cylinders in-line 4 valves per cylinder
Displacement	1998 cm ³
Bore × stroke	86 mm × 86 mm
Compression ratio	10.4
Valves diameters	Inlet: 32.8 mm Exhaust: 27.5 mm
Valves timings	IVO: 7 CAD BTDC IVC: 37 CAD ABDC EVO: 37 CAD BBDC EVC: 7 CAD ATDC
Valves lifts	Inlet: 9.2 mm Exhaust: 9.2 mm
Injection control	Bosch Motronic MP5.1
Injectors	Bosch 0280 155 216

(Bull Electric) operated as a dynamometer and the rotational speed was maintained constant to within 5 rpm by a controller (Shackleton Model 590). The engine and motor were secured to a test bed with vibration absorbers between the floor and the bed. The cooling water was circulated by an external pump through a heater and cooler and the temperature was maintained constant to within 2 °C at values from 50 to 95 °C by a proportional controller. The engine was lubricated by an internal oil pump.

The geometry of the combustion chamber is shown in Fig. 1 and cylinders 2, 3 and 4 were disabled by disengaging the inlet and exhaust valves from the camshaft, disconnecting their fuel injectors and removing their spark plugs to reduce the pumping work. Optical access to cylinder 1 was provided by introducing an annular ring of 30 mm thickness between the engine block and the cylinder head, with two optical windows, and an aluminium spacer of the same thickness around the three disabled cylinders, see Fig. 2. The two quartz windows had diameters of 19 mm and thickness of 8 mm with angular separation of 150° to facilitate measurements with the phase-Dropller velocimeter and were centered on the plane 15 mm below that of TCD. To compensate for the added thickness of the spacer and thereby to maintain the designed compression ratio of 10.4, the piston of cylinder 1 was extended by 30 mm and pistons of cylinders 2, 3 and 4 were weight balanced. The fuel pump, throttle, inlet and exhaust manifolds, catalytic converter and silencer were those provided with the production engine. Fuel was injected into the port

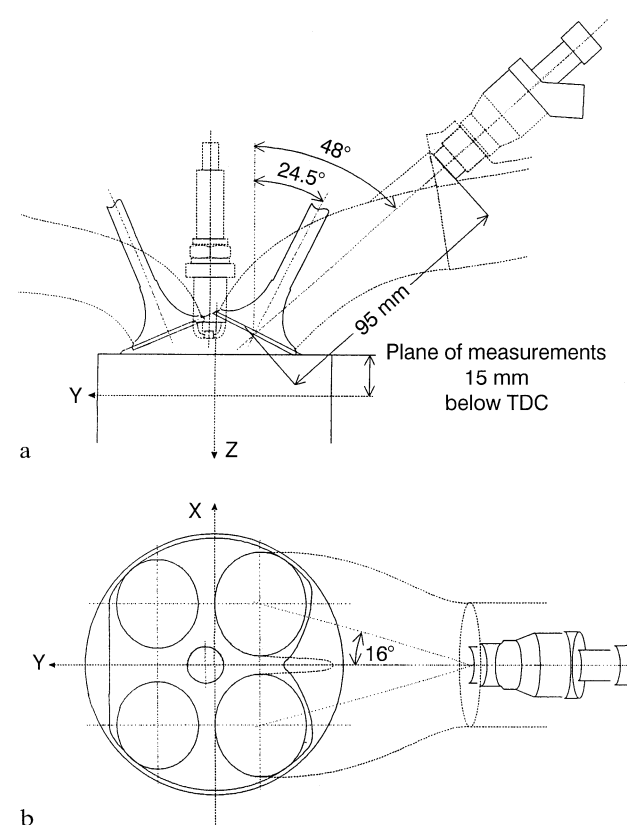


Fig. 1a, b. Geometry of the engine head. a vertical, b horizontal cross-sections

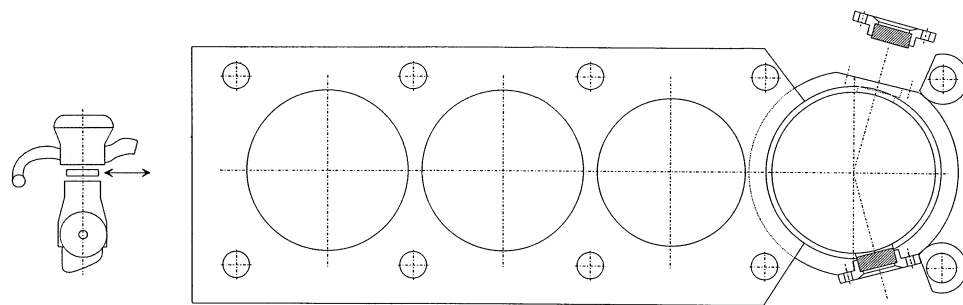


Fig. 2. Spacer, annular ring and optical windows

with a commercial gasoline injector (Bosch, type 0280 155 216) which delivered the fuel in two cones, each directed towards the head of an inlet valves and the engine management system (Bosch Motronic MP5.1) was replaced by a custom-built engine controller which allowed independent adjustment of the injection timing relative to the timing of the inlet valves.

An optical shaft encoder was coupled to the crankshaft and provided a sequence of pulses with angular resolution of 0.125 crank angles degrees. A magnetic pick-up was fixed to one of the camshafts to provide a reference reset pulse every 720 crank angles degrees. The signals from the shaft encoder were processed by the custom-built engine controller to control ignition and injection timing and to produce a time-base for the pressure and unburned hydrocarbon measurements and also for the phase-Doppler velocimeter.

The in-cylinder pressure traces were measured with a water-cooled pressure transducer (Kistler, type 7061) and a charge amplifier (Kistler, type 5007) was used to amplify the transducer output. The transducer "face" was coated with silicon rubber to eliminate thermal strain and it was calibrated according to procedure described by Lancaster et al. (1975). Concentrations of unburned hydrocarbons in the exhaust gases were measured with a fast FID system (Cambustion Ltd., model HFR 400), with a sampling probe located in the exhaust port about 25 mm from the valves. Condensation in the sampling probe was avoided by maintaining the temperature at 170°C with ohmic heating.

The output signals of the pressure transducer and fast FID system were interfaced to a microcomputer through a fast multi-channel A/D converter (Amplicon, type Dash-27) to obtain in-cylinder pressure and hydrocarbon concentrations simultaneously and as functions of crank angle. The maximum and mean-effective pressures were averaged from the pressure traces of 200 engine cycles and the concentrations of unburned hydrocarbon from a similar number and integrated over the exhaust stroke.

The phase Doppler velocimeter was similar to that of Posylkin et al. (1994) and Cousyn et al. (1995), based on that described by Hardalupas et al. (1989), and operated with an Argon-ion laser tuned to the green wavelength of 514.5 nm at a power of around 700 mW. The laser beam was transmitted by an optical fiber to the transmitting unit of the velocimeter. A rotating diffraction grating divided the laser beam and provided frequency shifts up to 4 MHz and a lens of 600 mm focal length focused the laser beams to the measurement location. The receiving optical unit was located at 30° to the plane formed by the incident light beams and the light

scattered by droplets was collected by a lens of 310 mm focal length and focused to a 50 μm slit, collimated and divided into three paths, each of which observed by a separate photomultiplier. The signals from the photomultipliers were processed by a custom-built counter, interfaced to a microcomputer to obtain simultaneously the velocity and size of droplets as a function of crank angle. The maximum frequency of the Doppler signal was around 5 MHz, leading to random values of uncertainties of velocity of up to 0.2 m/s and of size up to 2 μm which stemmed from the resolution of the 500 MHz internal clock of the phase-Doppler counter. The combination of transmitting and receiving optics during in-cylinder measurements resulted in a nominal measurement size range up to 180 μm. The characteristics of the phase-Doppler velocimeter are summarised in Table 2. The optical components for transmission and collection were mounted on supporting benches, separate from the engine and, to simplify traversing the bore of the cylinder, the benches were connected by a rigid link as shown in Fig. 3.

The main results were obtained at a rotational speed of 1200 rmp, 100 mbar manifold depression which corresponds to part load with 20° throttle opening at this engine speed and a steady-state water temperature of 85 °C. The duration of fuel injection was 11 ms, that is 82 CAD at 1200 rpm, and the volume of fuel delivered with each injection was 33 mm³ and corresponded to stoichiometric air-to-fuel ratio which was determined from the measurements of the air flow rate to the engine. The crank angle corresponding to the beginning of injection was varied from zero to 660 CAD after

Table 2. Characteristics of the phase-Doppler velocimeter

Ar ⁺ laser wavelength	514.5 nm
Beam diameter at e ⁻² intensity	1.25 mm
Frequency shift	3.129 MHz
Beam separation	27 mm
Half angle of beams intersection	1.283°
Dimensions of intersection volume at e ⁻² intensity	4.68 mm × 0.104 mm
Fringe spacing	11.491 μm
Number of fringes	9
Frequency to velocity conversion factor	0.087 MHz/ms ⁻¹
Focal length of collimating lens in receiving optics	310 mm
Separation between apertures 1 and 2	13.3 mm
Separation between apertures 1 and 3	26.7 mm
Phase to diameter conversion factor	0.502 μm/deg

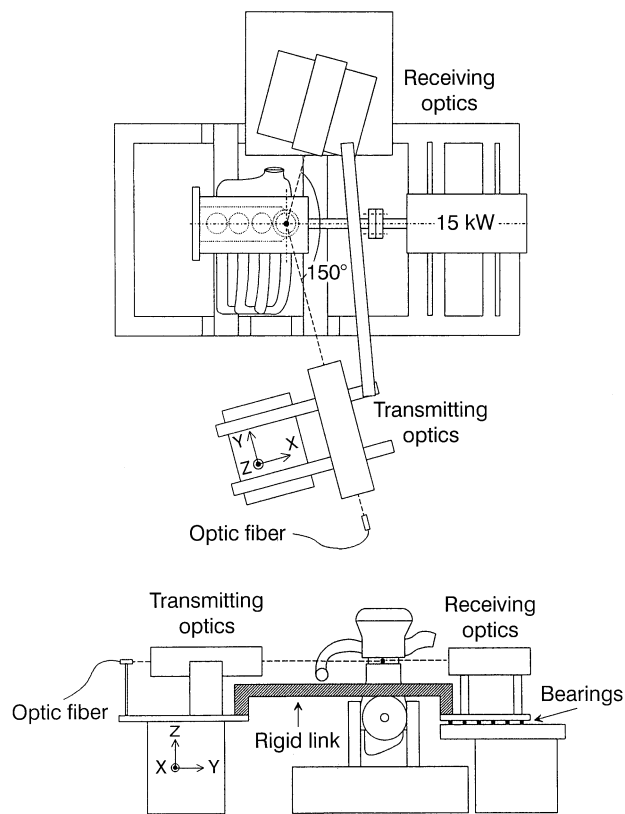


Fig. 3. Optical benches

top-dead-center of intake. Measurements were obtained with iso-octane (GPR 2,2,4-Trimethylpentane) rather than commercial gasoline since it led to less fouling of the windows.

Measurements of velocity and size were based, wherever possible, on at least 1000 samples, resulting in statistical uncertainties of less than 5% in the mean, 15% in the rms of the velocity signal and 5% in the cumulative size distribution based on the number of droplets (Tate, 1982). The liquid flux can be inferred, albeit with inaccuracy, from the data rates, direction of velocity vector and droplet diameters. The uncertainty of the timing circuit to assign a crank angle value to each datum was less than 0.13° based on resolution of the shaft encoder and the internal clock frequency of the phase-Doppler counter. The uncertainty of in-cylinder pressures, based on the 12 bit resolution of the A/D converter, was better than ± 1.5 mbar and of concentrations of unburned hydrocarbons, ± 30 ppm.

3

Presentation of results

The following two sections present the results of measurements of in-cylinder pressure and exhaust emissions of unburned hydrocarbon, and of the variation of droplet size, velocity and flux of the spray measured outside and inside the engine.

3.1

Performance

Figure 4 shows the consequences of injection timing in terms of cylinder pressures and concentrations of unburned

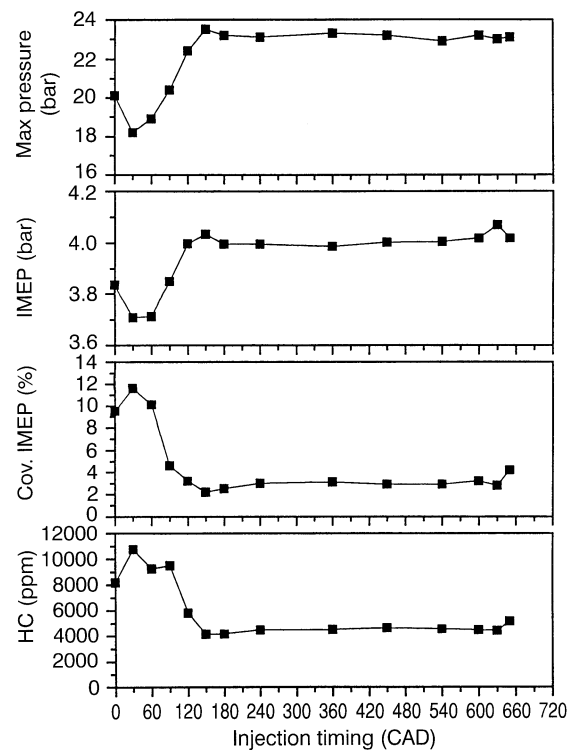


Fig. 4. Combustion performance and concentration of unburned hydrocarbons in the exhaust as a function of injection timing. Steady operating conditions with stoichiometric air/fuel ratio, 1200 rpm, 85°C water temperature

hydrocarbon in the exhaust gases. It is clear that there is a minimum in the maximum and mean-effective pressures with the beginning of fuel injection at 30° and 60° after the top-dead-center of intake and this corresponds to a maximum in the concentration of unburned hydrocarbons as would be expected. The variance of the mean-effective pressure is also a maximum at 60° after intake and corresponds to a reduction in drivability.

With injection over a wide range of crank angles corresponding to closed valves, there is little difference in the performance, except with injection at 645 CAD when an increase of about 2% in indicated mean-effective pressure was observed and was probably due to the interaction of the trailing edge of the injected spray with the back flow from the cylinder into the inlet port. As the start of injection was advanced to 660 CAD, performance decreased because the injection duration of 82 CAD and the time of flight from injector to the valves of about 5 ms implied that part of the spray entered the cylinder when the valves were open. Increase in engine speed with the start of injection at this crank angle led to injection of a larger proportion of the fuel with the valves open, since the time of flight from injector to the valves is independent of the rotational speed of the engine. The concentration of unburned hydrocarbon with closed-valve injection was about 4000 ppm, some 25% higher than expected in production SI engines, and probably due to the larger number of crevices associated with the extended piston and windows.

The above results indicate that, in common with previous studies in engines with four valves per cylinder which precluded the introduction of swirl, injection with the valves closed allowed time for evaporation of fuel prior to intake and created favorable conditions for combustion with consequently improved drivability and lower emissions of unburned hydrocarbons due to enhanced homogeneity of the mixture.

It is of interest that similar tests conducted with an injector which gave rise to a single hollow cone spray, rather than the dual sprays of the injector normally used in the engine, produced similar results to those of Fig. 4 with the single exception that the minimum in the indicated mean-effective pressures and the corresponding maximum in concentration of unburned hydrocarbons, observed with injection beginning at 60° after intake, were less pronounced. This may have been caused by smaller quantities of fuel entering the cylinder through the open valves, and with more fuel remaining on solid surfaces of the port to evaporate and enter the cylinder in the following intake stroke.

3.2

Droplet characteristics

3.2.1

Droplet characteristics measured in the free spray outside the engine

During a preliminary investigation, the spray was characterised in atmospheric air at a distance of 80 mm from the nozzle and Fig. 5 shows mean diameters, velocity and estimated liquid flux along the line passing through the centers of the cones. The axes of the two cones were separated by 30° and each cone had a 10° opening of a base area in which more than 90% of the liquid was concentrated. The two cones were full, rather than hollow as with the mono-jet injector, and the maximum Sauter mean diameter and velocity were $180 \mu\text{m}$ and 18 m/s respectively. The transient stage associated with the opening of the pintle lasted about 1 ms and there were no large droplets at the trailing edge of the spray. The size-velocity correlations, not shown here, indicated that velocities of large droplets were highest due to their momentum and longer relaxation times. The spatially-averaged Sauter mean diameter of the spray, weighted with the droplet data rate measured at about 70 locations within the spray cone, was around $130 \mu\text{m}$.

3.2.2

Effect of injection timing on droplet characteristics in the cylinder

The main measurements of droplet characteristics in the cylinder were obtained with the start of injection at zero and 60° CAD which corresponded to early and middle intake when the inlet valves were open and to 600° CAD with the valves closed. Since the combustion chamber and the intake port were symmetrical about the Y axis of Fig. 1, the measurements were limited to positive values of X and emphasised the flow from one inlet valve. The distributions of droplets within the cylinder were measured together with axial velocities V_Z and radial velocities V_X by the laser-Doppler velocimeter at twenty four locations along three lines from the inlet to the exhaust side and separated by 10 mm. The laser-Doppler velocimeter made use of light scattered in the forward direction to increase

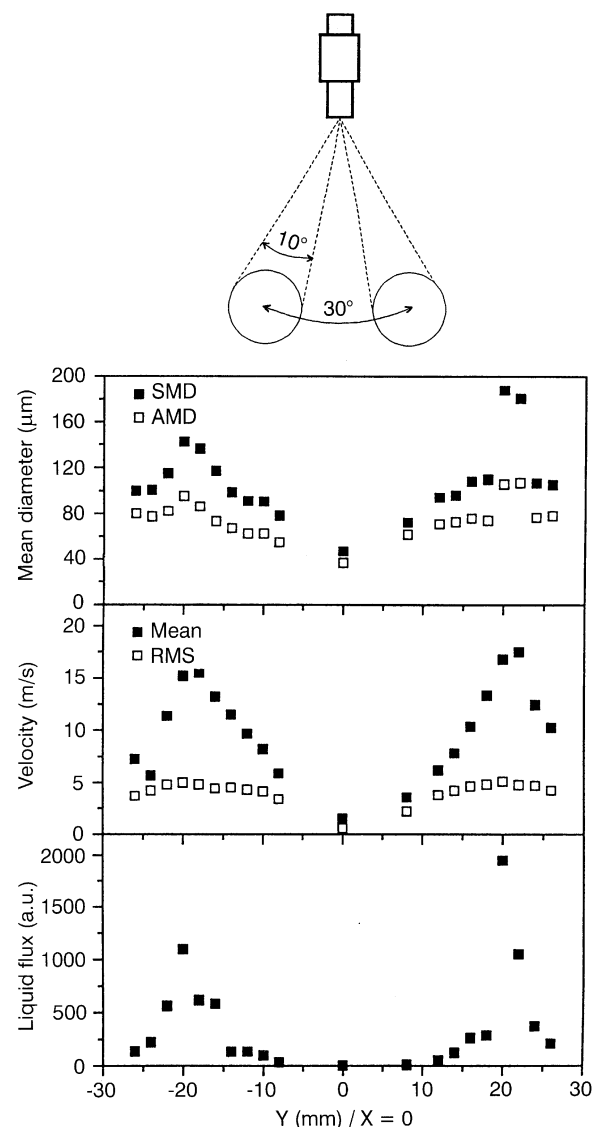


Fig. 5. Characteristics of the incident spray by a double-jet injector. Centre line profiles of mean diameters, velocity and liquid flux 80 mm from the nozzle. Injector type: Bosch 0280 155 216

signal quality and established the regions where the number of droplets was greatest. Droplet sizes and axial velocities were obtained subsequently with the phase-Doppler velocimeter and over a wider range of injection timings at two locations on the exhaust side, where the droplet concentration had been shown to be greatest, and below the spark plug to characterise the composition of the mixture as TDC of compression was approached. The plane of measurements, 15 mm below TDC, implied that optical access to the cylinder was blocked by the piston between 45° CAD before and after top-dead-centre.

Figure 6 presents the data rates at which droplets passed through the measurement locations for the three lines of measurement; the threshold level and logic of the counter were the same for all results presented. High data rates occurred on the exhaust side and close to the liner for all injection timings, and were highest with open-valve injection. It seems that most of the droplets entered the chamber from the inlet valves in

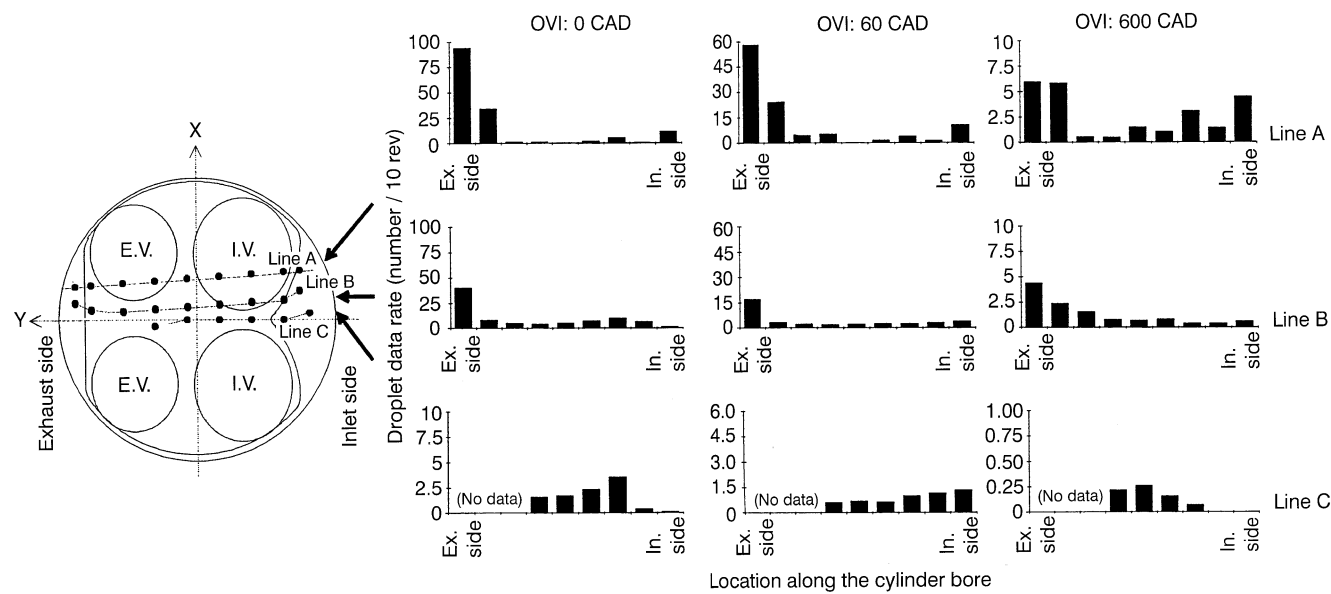


Fig. 6. Effect of the location on droplet data rates for three injection timings. Engine speed 1200 rpm, 100 mbar manifold depression and 85 °C cooling water temperature

a narrow cone directed towards the liner on the side of the exhaust valves and in common with the results of Posylkin et al. (1995b) in an isothermal simulation with a four-valve cylinder head and based on a larger number of measurement points across the cylinder bore. Most droplets were detected with injection at 0 CAD, approximately half this number with injection at 60 CAD and more than an order of magnitude fewer with injection at 600 CAD. These numbers should not be interpreted directly as fluxes since the smaller numbers of droplets may be associated with larger diameters as shown, for example, by Posylkin et al. (1994) and Cousyn et al. (1995) and confirmed by the measurements presented below for injection with the valves closed.

Figure 7a, b presents the temporal characteristics of droplet diameters and axial velocities for the three injection timings, at two locations close to the liner on the exhaust side and below the spark plug. Size velocity correlations are also shown at the location where the number of droplets was large. No droplets remained in the cylinder during the expansion and exhaust strokes. The number of droplets shown in Fig. 7 should not be interpreted as data rates since the duration of the measurement was different for these injection timings and two positions.

With injection with the valves open, the droplets inside the cylinder were detected with a time lag which corresponded to the time of travel from the injector to the measuring location. Thus, the first droplets were detected at about 70 CAD after the start of injection at the location close to the liner on the exhaust side, whereas they were detected below the spark plug after about 60 CAD due to the shorter distance from the injector. The droplets had Sauter mean diameters of about 40 μm at the locations close to the liner and nearly half that value under the spark plug and were almost the same for injection at zero and 60 CAD. These Sauter mean diameters were more than three times smaller than those of Fig. 5 and measured in free air outside the engine and, together with droplet size-velocity

correlations, imply impingement of the spray on the inlet valve and port surfaces and subsequent re-atomisation, as described by Posylkin et al. (1995a). The decrease in axial velocity of droplets with advance of injection timing from zero to 60 CAD is consistent with increase in the valve lift and decrease in the piston speed at the time of droplets passage through the valve gap. After the end of the intake stroke, and closure of the inlet valves, droplets with diameters of the order of 20 μm were observed to move upwards with the piston, consistent with the transport of smaller droplets by the tumble motion. The velocity measurements suggested that there was one rotation of the tumble vortex during the 360° of intake and compression and this led to droplets under the spark gap particularly with injection at 60 CAD, though with a small proportion of the injected fuel. The apparent large reduction in liquid flux is likely to stem from a combination of evaporation within the port and from impingement on the hot liner and the second is consistent with the measurements of Hardalupas et al. (1995) and the calculations of Nagaoka et al. (1994).

With injection with the valves closed, the droplets had time to settle on the hot surfaces of the port and valves so that small droplets were evaporated. Larger droplets, and those stripped from surfaces by the air flow, did not enter the cylinder immediately upon valve opening due to the back flow of hot residual gases from the cylinder into the inlet port. Inside the cylinder, most droplets were detected between 50 and 90 CAD and, although the Sauter mean diameter was around 110 μm , the total number was very much smaller than with open-valve injection. The size-velocity correlation shows that remaining small droplets were carried through the valve gap with velocities up to 20 m/s whereas the large droplets were associated with velocities of the order of 8 m/s. Droplets below the spark plug were similar in diameter to those measured with injection with the valves open but the number was smaller and almost no droplets survived to top-dead-centre of compression.

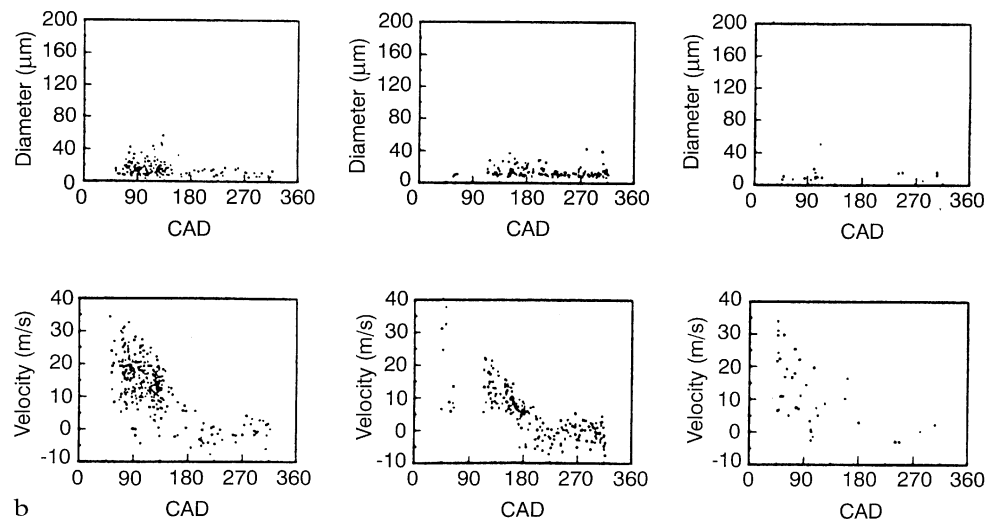
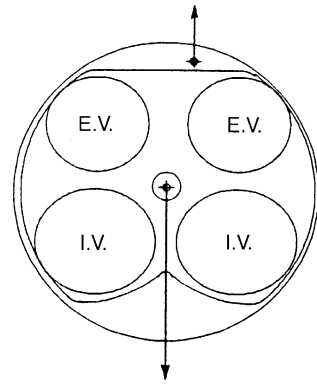
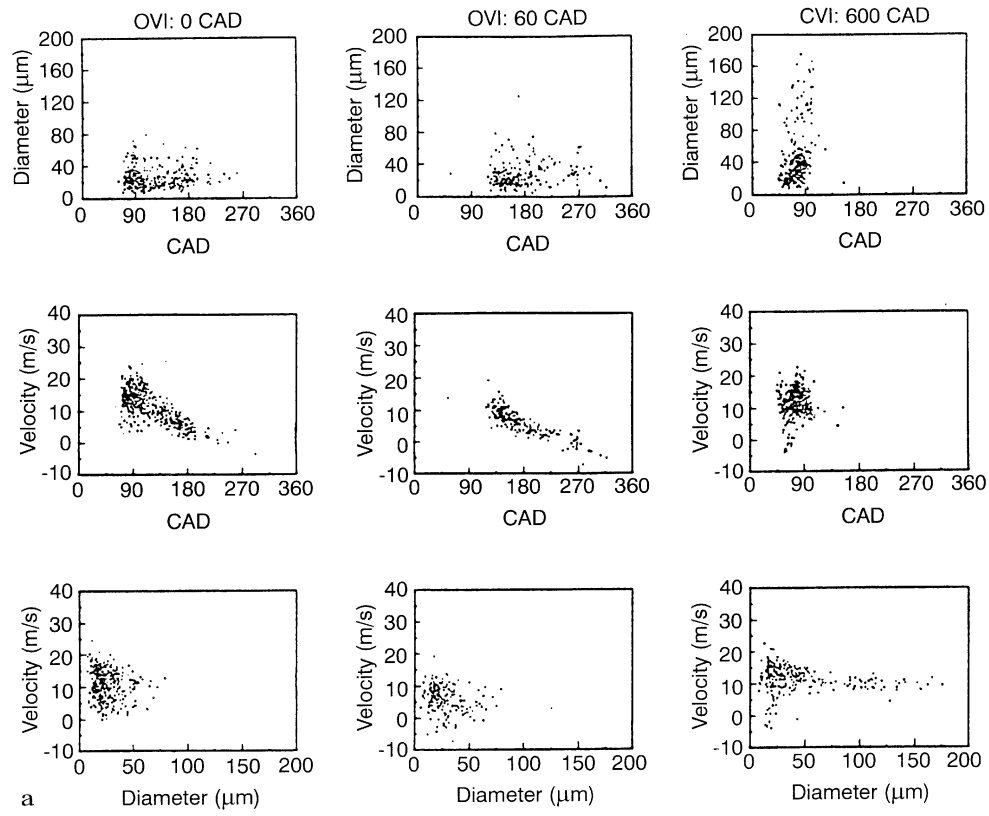


Fig. 7a, b. Droplet characteristics with three injection timings. **a** Location close to the liner; **b** location close to the spark plug. Engine speed 1200 rpm, 100 mbar manifold depression and 85 °C cooling water temperature

The radial velocities, not shown here, tended to be centered around zero and independent of injection timing, so that there was no dominant direction to provide convection of the droplets and this implies that the port did not induce swirl, as expected from its geometrical configuration. During valve opening up to about 100 CAD, there was a tendency for positive radial velocities in the region between the inlet valves which suggests interaction between the corresponding flows so that some of the droplets detected below the inlet valve may have originated from the second inlet valve, as well as from recirculation.

Figure 8 shows the effects of injection timing on droplet data rates and mean diameters for a wide range of the injection timings measured at the location of Fig. 7a, where most of the droplets crossed the plane of the measurements at intake. With injection with the valves open, droplet mean diameters did not change with injection delay from zero to 60 CAD and this suggests that the decrease in the local data rate with injection at 60° is likely to be associated mainly with the larger valve gap which allowed droplets to disperse over a wider region. With injection at 120 CAD, the time of flight from the injector to the valves implied that only droplets in the leading edge of the spray could enter the cylinder before the valves closed with the remainder settling on the valve. With injection with the valves closed, data rates decreased with increase in residence time prior to the opening of the valves since longer residence times of fuel on hot surfaces allowed more evaporation. With injection at 180 CAD, the residence time until intake was greatest so that the data rate was about 15 times smaller than

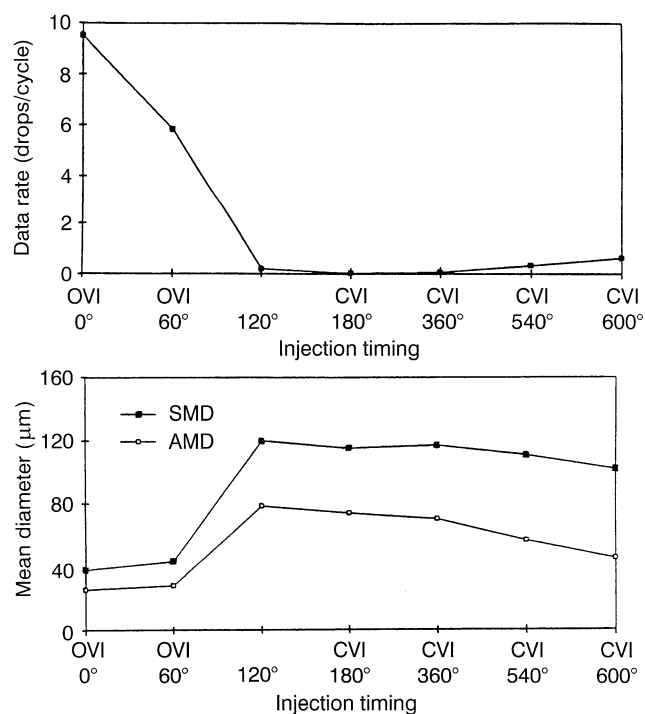


Fig. 8. Effect of injection timing on droplet data rates and mean diameters. Engine speed 1200 rpm, 100 mbar manifold depression and 85 °C cooling water temperature

with injection at 600 CAD. This change in data rate did not affect all droplets to the same extent and the proportion of small droplets decreased more with residence time as shown by the arithmetic mean diameter which increased from 45 to 78 μm whereas the Sauter mean diameter increased from 102 to 120 μm. With injection at 600 CAD, an estimate of the local flux in the cylinder, based on the product of the data rate and the averaged volume of fuel represented by the SMD³, is about half that with injection at zero degrees. The small contribution of the larger number of small droplets suggests, however, that above value may be overestimated and the ratio between the amount of liquid in the cylinder with closed and open valves injections was even smaller.

4 Discussion

Knowledge of the effects of injection timing on droplet characteristics in the cylinder is important because it provides a basis for subsequent mixture preparation at the time of ignition and links to the performance of the engine. The small number of droplets detected in the cylinder with injection with the valves closed suggests improved homogeneity of the mixture and it is clear that evaporation of fuel deposited on the hot surface of the inlet valves was aided by the back flow of the hot residual gases which occurred in the early stages of intake and has also been observed photographically by Shin et al. (1995) and Cousyn et al. (1997). The proportion of the fuel contained in the small number of large and slow moving droplets observed in the cylinder with these injection angles, was undoubtedly small compared to that in the vapor phase and few appeared to survive into the compression stroke. These effects are consistent with the near-constant performance with injection angles which corresponded to the closed inlet valves.

In contrast, most of the many droplets associated with injection with the valves open, and observed in the earlier stages of intake in the comparatively narrow region close to the liner on the exhaust side, had diameters and Stokes numbers that suggested impingement on the liner. The minima in the maximum and indicated mean-effective pressures and maximum in the covariance and the exhaust concentrations of unburned hydrocarbon may, therefore, have been caused by a region of rich mixture, partly in liquid form, which existed away from the spark plug at the time of ignition so that the flame kernel grew in a comparatively weak mixture.

The discussion of the previous paragraphs has some similarities with that of Hardalupas et al. (1995) and some important differences. The present engine was designed to operate with near-homogeneous and near-stoichiometric mixtures of fuel and air so that the presence of unevaporated fuel droplets was undesirable. Thus, for the conditions of the present experiments and probably for all steady-state conditions, injection with the valves closed is likely to be preferable, Injection through open valves and their operation so that swirl was absent led to impingement of the fuel on the liner at locations opposite to the inlet valves and, with tumble velocities which were not arranged to provide a region of rich mixture at the spark gap at the time of ignition, any stratification was not beneficial to flame propagation and led to poor performance as has been shown. In contrast, the engine of

Hardalupas et al. was designed to operate with a stratified charge and lean mixtures except at high load and stratification was obtained by a combination of open-valve injection and careful arrangement of the air flow so that the flame kernel was established in a region of comparatively rich mixture before propagating through the leaner mixture. It should be recognised, however, that lean-burn with port injection is likely to have limitations so that some degree of direct injection, as for example by Arcoumanis et al. (1996), may be required to allow satisfactory performance at air–fuel ratios in excess of around 30.

5

Summary, conclusions

The performance and in-cylinder droplet characteristics of a sixteen-valve, four cylinder engine operating with combustion in one cylinder have been measured as a function of injection timing at 1200 rpm, part load and stoichiometric mixture of gasoline and air. The following is the summary of the more important conclusions:

1. Injection with the valves closed Performance of the engine in terms of indicated mean-effective pressure, drivability and emissions of unburned hydrocarbon was found to be nearly constant with the initiation of injection from 150 to 630 CAD and indicated good homogeneity of the mixture. With the onset of injection at these crank angles, some droplets in the cylinder were formed by stripping of the liquid films from the valve and port surfaces and led to Sauter mean diameters of the order of 110 μm . The number of droplets entering the cylinder was much reduced with injection at crank angles corresponding to closed valves due to evaporation, which was facilitated by the back flow of the hot residual gases from the cylinder into the intake port at the early stages of intake, and the few large droplets which emerged did not survive to top-dead-centre of compression.

2. Injection with the valves open About 10% reduction in indicated mean-effective pressure, poor drivability and concentrations of unburned hydrocarbon of up to 11000 ppm were measured with injection corresponding to open inlet valves. At these injection angles, large numbers of droplets entered the cylinder and most were detected close to the liner on the side of the exhaust valves and had Sauter mean diameters of the order of 40 μm and axial velocities of up to 40 and 20 m/s for injection at zero and 60 CAD, respectively. Most of these droplets had high probability of impingement on the liner, with some of the smaller droplets were convected by the tumbling vortex to the inlet side of the cylinder towards the end of the compression stroke. It is likely that these droplets, together with a region of a rich mixture close to the liner, led to an inhomogeneous mixture with the resulting poorer flame front propagation responsible for the reduction in performance.

References

- Alkidas AC (1994) The effects of fuel preparation on hydrocarbon emissions of a S.I. engine operating under steady-state conditions. SAE Paper 941–1959
- Arcoumanis C; Hu Z; Vafidis C; Whitelaw JH (1991) Tumbling motion: a mechanism for turbulence enhancement in spark-ignition engines. SAE Paper 900060
- Arcoumanis C; Hull DR; Whitelaw JH (1994) An approach to charge stratification in lean-burn, spark-ignition engines. SAE Paper 941878
- Arcoumanis C; Hull DR; Whitelaw JH (1996) Optimising local charge stratification in a lean-burn spark-ignition engine. Proc I Mech E (to be published)
- Bandel W; Fraidl GK; Mikulic L; Carstensen H; Quissek F (1989) Investigation of mixture preparation and charge motion effects on the combustion of fast-burn gasoline engines. SAE Paper 890160
- Cousyn B; Neveu F; Posylkin M; Whitelaw DS; Whitelaw JH (1997) Spray characteristics in the port and cylinder of a four-valve spark-ignition engine. In: Development in laser techniques and fluid mechanics, Vol. 8 ed. Adrian et al. Berlin: Springer. To be published
- Cousyn B; Posylkin M; Vannobel F; Whitelaw JH (1995) Droplet characteristics in two cylinders of a firing spark-ignition engine. SAE Paper 952466
- Hardalupas Y; Taylor AMKP; Whitelaw JH (1989) Velocity and particle flux characteristics of turbulent particle-laden jets. Proc Roy Soc 426: 31–78
- Hardalupas Y; Taylor AMPK; Whitelaw JH; Ishii K; Miyano H; Urata Y (1995) Influence of injection timing on in-cylinder fuel distribution in a Honda VTEC-E engine. SAE Paper 950507
- Horie K; Nishizawa K; Ogata T; Akazaki S; Miura K (1992) The development of a high fuel economy and high performance four-valve lean-burn engine. SAE Paper 920455
- Lancaster DR; Krieger RB; Lienesch JH (1975) Measurement and analysis of engine pressure data. SAE Paper 750026
- Mikulic L; Quissek F; Fraidl GK (1990) Development of low emission high performance four-valve engines. SAE Paper 900227
- Nagaoka M; Kawazoe H; Nomura N (1994) Modeling fuel spray impingement on a hot wall for gasoline engines. SAE Paper 940525
- Posylkin M; Taylor AMKP; Vannobel F; Whitelaw JH (1994) Fuel droplets inside a firing spark-ignition engine. SAE Paper 941989
- Posylkin M; Taylor AMKP; Whitelaw JH (1995a) Manifold injection and origin of droplets at the exit of an inlet valve. In: Developments in laser techniques and applications to fluid mechanics, ed. Adrian et al., Vol. 7, pp 132–146. Berlin: Springer
- Posylkin M; Taylor AMKP; Whitelaw JH; Ishii K; Miyano M (1995b) Measurement of droplet velocity and size downstream of the moving valves of a four-valve engine with manifold injection, operated under isothermal steady suction conditions. ASME – Internal Combustion Engine Division Spring Technical Conference, 23–26 April, Marietta, OH. Paper 95-ICE-10
- Shin Y; Min K; Cheng WK (1995) Visualisation of mixture preparation in a port-fuel injection engine during engine warm-up. SAE Paper 952481
- Tate RW (1982) Some problems associated with the accurate representation of droplet size distributions. Proc. 2nd Int. Conf. on Liquid Atomisation and Spray Systems (ICLASS), Wisconsin, USA
- Vannobel F; Robart D; Dementhon JB; Whitelaw JH (1994) Velocity and size distributions of fuel droplets in the cylinder of a two-valve production spark-ignition engine. Proc. 3rd Int. Symp. on Diagnostics and Modeling of Combustion in Internal Combustion Engines COMODIA-94, 11–14 July, Yokohama, Japan, pp 371–378
- Winklhofer E; Fraidl GK; Plimon A (1982) Monitoring of gasoline fuel distribution in a research engine. Proc I Mech 206: 107–115